J Mol Model (2013) 19:4815–4822
DOI 10.1007/s00894-013-1977-7

ORIGINAL PAPER

Theoretical investigation on the kinetics and branching ratio of the gas phase reaction of sevoflurane with Cl atom

Hari Ji Singh · Nand Kishor Gour · Pradeep Kumar Rao · Laxmi Tiwari

Received: 8 June 2013 / Accepted: 21 August 2013 / Published online: 11 September 2013

Abstract The present work deals with the theoretical investigation on the Cl initiated H-atom abstraction reaction of sevoflurane, $(CF_3)_2CHOCH_2F$. A dual-level procedure has been adopted for studying the kinetics of the reaction. Geometrical optimization and frequency calculation were performed at DFT(BHandHLYP)/6-311G(d,p) while single-point energy calculation was made at CCSD(T)/6-311G(d,p) level of theory. The intrinsic reaction coordinate (IRC) calculation has also been performed to confirm the smooth transition from the reactant to product through the respective transition state. The rate constants were calculated using conventional transition state theory (TST). It has been found that 99 % of the reaction proceeded via the H-atom abstraction from the $–CH_2F$ end of the sevoflurane. The rate constant of the dominant path is found to be 1.13×10^{-13} cm^3 $molecule^{-1}$ s^{-1}. This is in excellent agreement with the reported experimental rate constant of 1.10×10^{-13} cm^3 $molecule^{-1}$ s^{-1} obtained by relative rate method using FTIR/Smog chamber and LP/LIF techniques.

Keywords Sevoflurane · BHandHLYP · Branching ratio · CCSD(T) · IRC

Introduction

Oxygenated volatile organic compounds (OVOCs) are emitted in the atmosphere from numerous biogenic and anthropogenic sources. These species may also be produced during the tropospheric reactions of other volatile organics present in the atmosphere [1–5]. The presence of such species has led to serious concerns about the increasing risk to human health. The increase of atmospheric concentration of these halogenated organic compounds is partially responsible for a change in the global climate. Some halogenated organic ethers such as isoflurane ($CF_3CHClOCHF_2$), desflurane ($CF_3CHFOCHF_2$) and sevoflurane, $(CF_3)_2CHOCH_2F$ are inhalable anaesthetics mainly used in medical settings for induction and maintenance of general anaesthesia. These anaesthetics are highly volatile and chemically stable and once emitted in the atmosphere can remain there for a long time. Annual global emission of these volatile anaesthetic agents (VAA) to the atmosphere is not well known, but a recent study estimated it to be in the range of several kton/year [6]. It is certain that, in comparison to other major halocarbons such as chlorofluro- and hydrochloroflurocarbons, the current atmospheric level of these anaesthetics only make a minor contribution to the atmospheric pollution. However, there is a need for the understanding of the atmospheric degradation mechanism of the above mentioned VAAs. Out of the three mentioned above, the atmospheric degradation of isoflurane ($CF_3CHClOCHF_2$) has been studied by Wallington et al. [7] and the fate of the molecule and its peroxy radical formed as a result of the reaction of OH and Cl is discussed in the light of atmospheric chemistry. Recently an experimental study has been performed to study the kinetics of OH and Cl initiated reactions of $CF_3CHClOCHF_2$, $CF_3CHFOCHF_2$ and $(CF_3)_2CHOCH_2F$ by Sulbaek Andersen et al. [8] employing Smog chamber/FTIR and LP/LIF techniques. Using relative rate method the rate constants of various channels were calculated and their atmospheric implications have been discussed.

It is known that Cl atom and its oxides react faster than OH radical and can play an important role in the destruction of volatile organics in the atmosphere especially in the marine boundary layer and in polar regions where the concentration of Cl atoms is higher than other regions of the earth atmosphere [9]. The average global concentration of Cl atom in the atmosphere has been estimated to be 10^4 atom/cm^3 [10]. Therefore,

H. J. Singh (✉) · N. K. Gour · P. K. Rao · L. Tiwari
Department of Chemistry, DDU Gorakhpur University, Gorakhpur 273 009, India
e-mail: hjschem50@gmail.com

Cl initiated reactions may play a significant role in the degradation of many VOCs in the atmosphere. The gas-phase H-atom abstraction reactions of Cl atoms with H-containing halocarbons lead to the formation of facile radicals which also play an important role in atmospheric chemistry. Several DFT studies have been performed on sevoflurane molecule but none of these dealt with its kinetics and degradation process of sevoflurane. Freitas et al. [11] studied the stereoelectronic interactions and the coupling of C-F bond in sevoflurane while Lesarri et al. [12] dealt with the conformational analysis of the titled compound and reported the optimized parameters of the stable conformation on its potential energy surface. Tang et al. [13] reported the electronic structure properties of sevoflurane at HF and B3LYP methods utilizing 6-311+G(2d,p) basis set. These results will be compared with the data obtained during the present study. Literature survey reveals that considerably less attention has been directed toward the study of kinetics and mechanism of Cl-initiated H-atom abstraction reactions of halocarbons under atmospheric conditions. We find only one experimental study [8] that has been performed on the H-atom abstraction by Cl from sevoflurane and the overall rate constant determined using relative rate method has been found to be 1.10×10^{-13} cm^3 $molecule^{-1}$ s^{-1}. Sevoflurane possesses H atoms under two different environments and therefore the relative rate method will not be able to figure out the dominant pathways of the abstraction reactions. With this view point the present study has been undertaken and an attempt has been made to find the dominant pathways and the branching ratio of H-atom abstraction from sevoflurane by Cl atoms. The reaction of Cl atom with $(CF_3)_2CHOCH_2F$ (sevoflurane) is envisaged to proceed via hydrogen atom abstraction either from $–CH_2F$ site or –CHO site and the resulting two primary processes are designated as follows:

$$(CF_3)_2CHOCH_2F + Cl \rightarrow (CF_3)_2COCH_2F + HCl \quad (R1)$$
$$(CF_3)_2CHOCH_2F + Cl \rightarrow (CF_3)_2CHOCHF + HCl \quad (R2)$$

In the present work, our aim is to find out the contribution of the individual channel to the overall rate constant and to provide an understanding of the kinetics involved in the reactions R1 and R2. In order to do so a dual-level procedure, i.e., the geometry optimization and the frequency calculation was performed at a low level and the single-point energy calculation was made at a higher level as proposed by Truhlar and co-workers [14–16]. Thus, the optimization and frequency calculation was performed at DFT using hybrid density functional BHandHLYP [17] with 6-311G(d,p) basis set followed by a single-point energy calculation at CCSD(T) level [18]. This dual level procedure is denoted as CCSD(T)//BHandHLYP/6-311G(d,p). The thermodynamic and kinetic data are obtained and the results are compared with the experimental data. The branching ratio of the two reaction channels are also determined. Potential energy diagram is constructed using the refined energy data obtained at CCSD(T) level.

Computational details

The geometries of reactant, products and transition states involved in the reaction channels R1 and R2 were optimized at DFT using hybrid density functional (BHandHLYP) with 6-311G(d,p) basis set. In order to determine the nature of stationary points on the potential energy surface, vibrational frequencies calculation was made using the same level of theory at which the optimization was made. All the electronic calculations were performed using GAUSSIAN 09 program package [19]. The stationary points were identified to correspond to stable minima on the respective potential energy surface by ascertaining that all the harmonic vibrational frequencies were real and positive. The transition states in reactions R1 and R2 were obtained using synchronous transition-guided quasi-Newton (STQN) method [20, 21] and the first order saddle point was characterized by the presence of only one imaginary frequency (NIMAG=1). IRC calculations were also performed in order to ascertain that the transition of reactants to products via corresponding transition state was smooth. The minimum energy path (MEP) was obtained by intrinsic reaction coordinate (IRC) calculation performed using Gonzales-Schelgel steepest descent path in mass-weighted Cartesian with a gradient step-size of 0.05 $(amu)^{1/2}$-bohr [22, 23]. Bond dissociation energy (BDE) is an important parameter in understanding the progress of a chemical reaction. In principle, the reaction enthalpy for the homolytic dissociation of $(A—B)_{(g)} \rightarrow A^{\bullet}_{(g)} + B^{\bullet}_{(g)}$ at 298 K and 1 atm is termed bond dissociation enthalpy of the bond in the molecule AB [24]. Bond dissociation energy (BDE) and bond enthalpy are interchangeably used in the literature for showing the bond strength in organic molecules. Thus, BDE of C-H bonds involved during reactions R1 and R2 were calculated in terms of Eq. 1:

$$BDE_0(A{-}B) = E_0(A^{\bullet}) + E_0(B^{\bullet}) - E_0(A{-}B), \quad (1)$$

where E_0's are the zero-point corrected total energy of the corresponding species. $A^{\bullet}$ and $B^{\bullet}$ are the radical species formed as a result of homolytic fission of the covalent bond.

Results and discussion

Electronic structure

The electronic structure of reactants [$(CF_3)_2CHOCH_2F$, Cl], products [$(CF_3)_2COCH_2F$, $(CF_3)_2CHOCHF$, HCl] and transition states TS1 and TS2 optimized at BHandHLYP/6-311G(d,p) level of theory are shown in Fig. 1 and the bond distances of the optimized structure of the sevoflurane are recorded in Table 1 that also lists the values obtained by Tang et al. [13] at HF and B3LYP utilizing 6-311+G(2d,p) basis set and by Lesarri et al. [12] at MP2/6-311++G(2df,p) level. The results show that the bond distances of the titled molecule obtained during the present study at BHandHLYP/6-311G(d,p) level are closer to the values obtained at MP2 level reported by Lesarri et al. [12]. MP2 values for C2-H1 and C4-

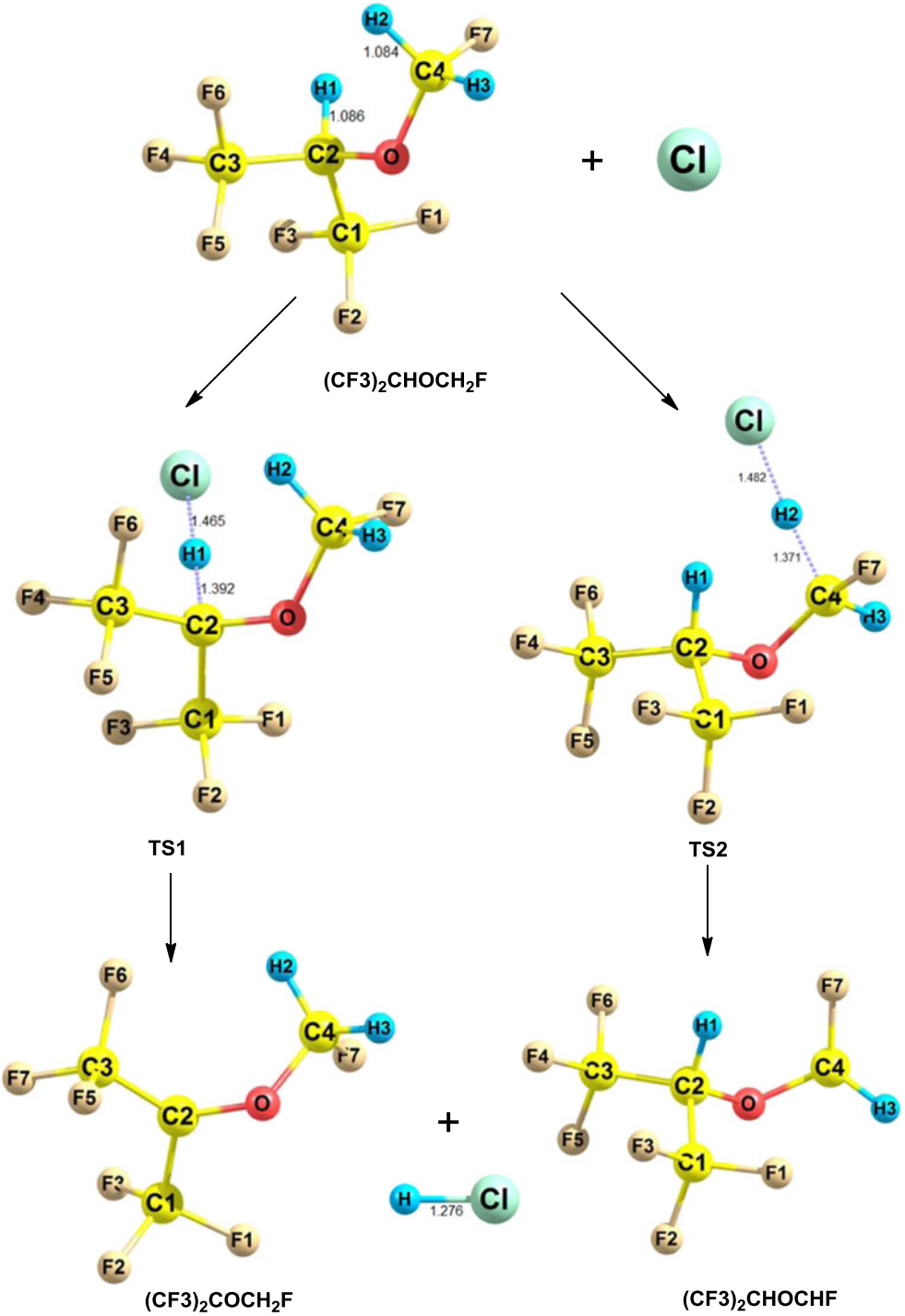

Fig. 1 Optimized geometry of reactants, products and transition states at BHand HLYP/6-311G(d,p) level

Table 1 Bond lengths of geometry-optimized sevoflurane. Values are in (Å)

Bond length	*HF/6-311+G(2d,p)	*B3LYP/6-311+G(2d,p)	**MP2/6-311++G(2df,p)	#BHandHLYP/6-311G(d,p)	Experimental$
C1-F1	1.310	1.341	1.327	1.322	1.340±0.019
C1-F2	1.306	1.335	1.327	1.320	
C1-F3	1.317	1.351	1.342	1.327	
C3-F4	1.309	1.340	1.335	1.324	
C3-F5	1.307	1.337	1.331	1.318	
C3-F6	1.312	1.344	1.329	1.332	
C1-C2	1.526	1.539	1.526	1.522	1.526±0.028
C3-C2	1.526	1.538	1.526	1.523	
C2-O	1.383	1.408	1.403	1.393	1.410±0.026
O-C4	1.373	1.392	1.389	1.379	
C4-F7	1.351	1.387	1.375	1.363	1.390
C2-H1	1.083	1.093	–	1.086	1.095±0.011
C4-H2	1.076	1.088	–	1.084	
C4-H3	1.080	1.091	–	1.080	

*Values taken from Tang et al. [13]

**Values given by Lesarri et al. [12]

Present study

$ Average bond distance taken from CRC Handbook of Physics and Chemistry [25]

H2 that are involved in the abstraction processes R1 and R2 are not reported by Lesarri et al. [12], however, our results for these two bonds are very close to the values calculated at B3LYP/6-311+G(2d,p) by Tang et al. [13]. The bond distances of the optimized structure of sevoflurane calculated during the present study are also close to the experimental values reported by Tang et al. [13] that are obtained by taking into account the average value of the data available in the literature [25]. However, our interest in the present study has been directed toward the kinetics of H-atom abstraction process and therefore, we concentrated more on the transition state structures TS1 and TS2 involved during the abstraction process. The distances of the bonds involved during the transition states are noted on the corresponding optimized structures shown in Fig. 1 and compared with the values of the parent molecule sevoflurane as listed in Table 1. The results show that the breaking bonds C2-H1 in TS1 stretches from 1.086 Å to 1.392 Å and C4-H2 in TS2 from 1.084 Å to 1.371 Å. The elongation of breaking bonds in the transition states TS1 and TS2 corresponding to reactions R1 and R2 is about 28 % and 27 % respectively when compared with the corresponding equilibrium bond distances in the isolated sevoflurane molecule. On the other hand, stretching of the forming H—Cl bond in transition states TS1 and TS2 is about 15 % (1.276 Å-1.465 Å) and 16 % (1.276 Å −1.482 Å) than the equilibrium bond distance of 1.276 Å in the HCl molecule. These results show that the extent of elongation in the newly forming H-Cl bond (15-16 %) is lower than that of the breaking C-H bond (27-28 %) in both cases. Consequently, TS1 and TS2 can be considered as a late barrier and the transition states would be product like envisaging thereby that both reactions R1 and R2 will proceed through late transition states. This is consistent with the view expressed by Fischer and Radom [26] that endothermic reaction proceeds via "late" transition state and exothermic reaction occurs through "early" transition state. This is supported by the data recorded in Table 2 showing thereby that both reactions R1 and R2 are endothermic by about 3 kcal mol^{-1}. This perspective has been shown by Sun et al. [27] and Song et al. [28] during their theoretical studies performed on the reactions of OH radicals on other haloethers.

The normal mode harmonic vibrational frequencies of all the species involved in reactions R1 and R2 are calculated at BHandHLYP/6-311G(d,p) level of theory and these are listed in Table 3. The imaginary frequencies in TS1 and TS2 are found to be 1407 cm^{-1} and 1085 cm^{-1} respectively. Visualization of these imaginary frequencies with GaussView [30] yielded a qualitative view of the transition states connecting the reactant and products. The existence of the transition state on the potential energy surface, however, is ascertained by intrinsic reaction coordinate (IRC) calculation performed at the same level. The IRC plots for TS1 and TS2 as shown in Fig. 2 which clearly depicts a smooth transition from reactant to product through the respective transition state on the corresponding potential energy surface.

Spin contamination was not an issue for the radicals formed during the progress of reaction channels R1 and R2 because $< S^2 >$ for the radicals was found to be 0.76 before annihilation which is only slightly larger than the expected value of $< S^2 > = 0.75$ for doublets.

Table 2 Thermochemical data for reaction channels R1 and R2 calculated CCSD(T) level. The values are in kcal mol^{-1} at 298 K

Reaction channels	$\Delta G^{\#}$	$\Delta_r G°$	$\Delta_r H°$
Reaction, R1	15.8	−0.60	3.0
Reaction, R2	10.1	−0.74	2.2

Table 3 Unscaled vibrational frequencies of reactant, products and transition states calculated at BHandHLYP/6-311G (d,p) level of theory

Species	Vibrational frequency (cm^{-1})
$(CF_3)_2CHOCH_2F$	36, 48, 70, 107, 166, 195, 231, 305, 308, 343, 375, 466, 543, 560, 574, 600, 632,723, 780, 929, 957, 1095, 1115, 1185, 1205, 1249, 1259, 1299, 1320, 1351, 1364, 1387, 1466, 1485, 1519, 1590, 3163, 3181, 3255.
TS1	***1407i***, 27, 53, 59, 73, 77, 85, 161, 173, 227, 299, 303, 308, 341, 370, 464, 549, 559, 562, 576, 645, 733, 792, 895, 936, 1020, 1055, 1074, 1158, 1215, 1251, 1275, 1284, 1313, 1335, 1364, 1398, 1418, 1527, 1585, 3203, 3282.
TS2	***1085i***, 16, 24, 58, 70, 107, 138, 169, 138, 169, 187, 228, 298, 305, 341, 368, 438, 483, 548, 561, 576, 618, 654, 726, 783, 928, 954, 1024, 1048, 1084, 1188, 1200, 1255, 1270, 1293, 1301, 1342, 1344, 1384, 1433, 1464, 1478, 3201, 3245.
$(CF_3)_2COCH_2F$	24, 36, 46, 71, 131, 157, 231, 306, 307, 342, 360, 466, 525, 564, 570, 582, 633, 7167, 738, 808, 1033, 1084, 1139, 1205, 1214, 1244, 1252, 1282, 1327, 1359, 1434, 1476, 1532, 1588, 3186, 3270.
$(CF_3)_2CHOCHF$	29, 38, 67, 88, 155, 184, 238, 276, 308, 343, 357, 465, 542, 561, 575, 618, 646, 720, 781, 920, 947, 961, 1091, 1189, 1210, 1254, 1275, 1297, 1325, 1354, 1377, 1396, 1457, 1482, 3210, 3245.
HCl	3046 [2991][a]

[a] Experimental value taken from ref [29]

Energetics

Thermodynamic properties like reaction enthalpy (Δ_rH) and Gibbs free energy (Δ_rG) change and free energy of activation ($\Delta G^{\#}$) for reactions R1 and R2 calculated from the single-point energy data obtained at CCSD(T)/6-311G(d,p) level are listed in Table 2. Results show that both R1 and R2 are exergonic ($\Delta G<0$). The calculated enthalpy change shows that both channels are endothermic by 3.0 kcal mol^{-1} and 2.2 kcal mol^{-1} respectively. Bond dissociation energy (BDE) of the C-H bond calculated using Eq. (1) from two different sites –CHO and $–CH_2F$ in the sevoflurane molecule are found to be 98.4 kcal mol^{-1} and 97.7 kcal mol^{-1} respectively. The results show that C-H bond of the $–CH_2F$ site is 0.7 kcal mol^{-1} lower than that of the –CHO site. These results show that reaction R2 would be energetically more favorable in comparison to R1. Zero-point corrected total energies for various species and transition states involved and the associated energy barriers for the reaction channels R1 and R2 are shown in Table 4. An energy level diagram is constructed as shown in Fig. 3 by taking the ground state energy of the reactants $(CF_3)_2CHOCH_2F$ + Cl, arbitrarily as zero. The energy barriers for R1 and R2 are found to be 8.8 and 3.4 kcal mol^{-1}. This also shows that reaction R2 is the dominant path. In conclusion we find that R2 is kinetically and thermodynamically the dominant path amongst the two possible H-atom abstraction reactions considered.

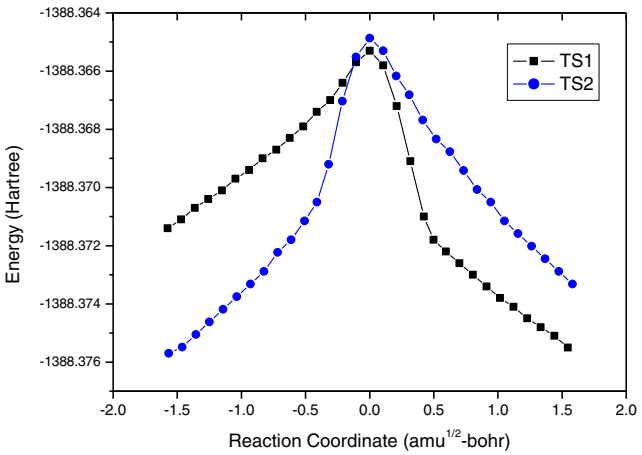

Fig. 2 IRC plots of transition states for reaction channels R1 and R2 obtained at BHandHLYP/6-311G(d,p) level

Rate constant and branching ratio

The conventional transition state theory (TST) [31, 32] has been used to calculate the rate constant for the H-atom abstraction reactions of sevoflurane by Cl atom. Both reaction channels R1 and R2 proceed with positive energy barrier and therefore, the reactions are envisaged to occur via a direct mechanism (Reactant → TS → Product). In such cases, the rate constant can conveniently be evaluated by using transition state theory written as:

Table 4 Zero-point corrected total energy, E of reactant, product and transitions states and the associated energy barrier for reactions R1 and R2. The data are obtained at CCSD(T) level

Species	E (Hartree)	ΔE_0 (kcal mol^{-1})
$(CF_3)_2CHOCH_2F$ + Cl	−1386.177408	0.0
TS1	−1386.163429	8.8
TS2	−1386.172018	3.4
$(CF_3)_2COCH_2F$ + HCl	−1386.173943	2.2
$(CF_3)_2CHOCHF$ + HCl	−1386.175088	1.5

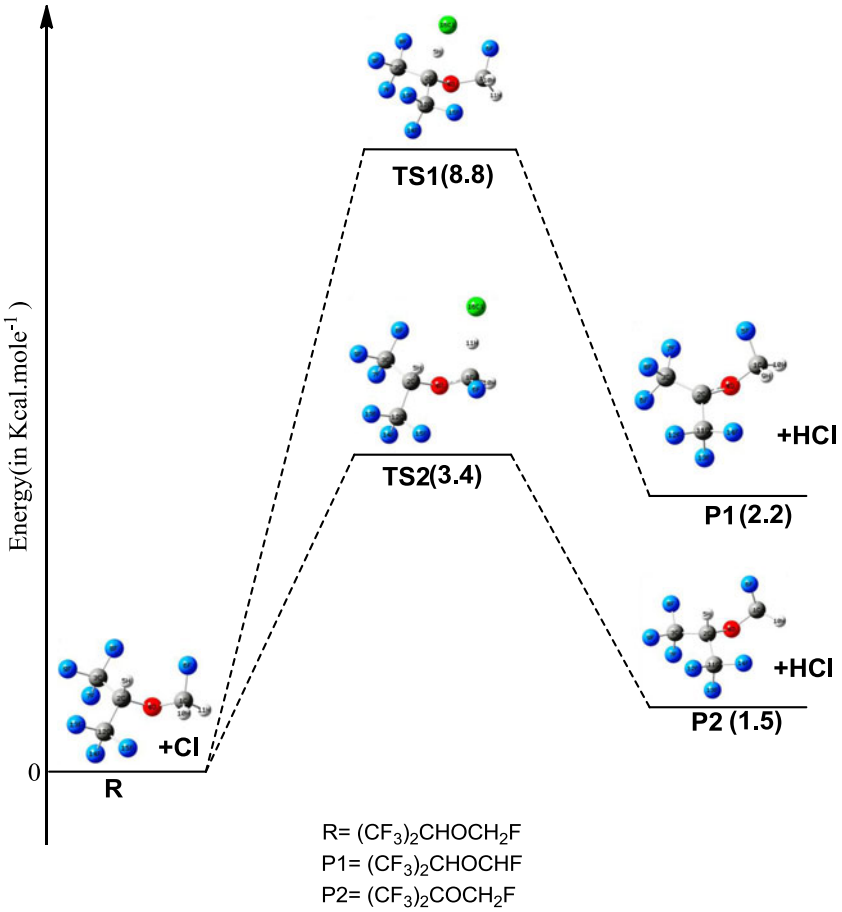

Fig. 3 Energy level diagram for reaction of sevoflurane with Cl atom at CCSDT/6-311G(d,p) level. Values are in kcal mol^{-1}

$$k = \Gamma(T)\frac{k_B T}{h}\frac{Q^{\ddagger}_{TS}}{Q_R}\exp\frac{-\Delta E_0}{RT}, \quad (2)$$

where $\Gamma(T)$ denotes tunneling correction factor at temperature T, $Q^{\ddagger}_{TS}$ and Q_R are the total partition functions of transition state and reactant respectively. ΔE_0 is the barrier height and other terms have their usual meaning. Tunneling is important in reactions where the light mass atom such as H is involved in the migration during the progress of the reaction. Both reaction channels considered above involve the transfer of H atom and therefore, tunneling correction factor needs to be evaluated. The tunneling correction factor $\Gamma(T)$ was calculated using Wigner's empirical method [33] given by the following expression:

$$\Gamma(T) = 1 + \frac{1}{24}\left(\frac{h\nu^{\#}}{k_B T}\right)^2, \quad (3)$$

where $\nu^{\#}$ is the imaginary frequency obtained during the frequency calculation on the optimized geometry of the transition state. The calculated Γ(T) values for R1 and R2 are found to be 2.9 and 2.1 respectively.

The total partition functions of reactant and transition states involved in the rate constant calculation using Eq. (2) were corrected for internal rotation (hindered and free rotors). Four low frequencies (36, 48, 70 and 107) in sevoflurane molecule were identified as internal rotors during hindered rotor calculation performed using G09 program. Careful examination of these vibrations using Gauss-View [30] reveals that out of the above listed four frequencies, only one at 36 cm^{-1} involving a rotational barrier of 2.25 kcal mol^{-1} can be taken as hindered rotor and the remaining three frequencies would behave as normal vibrational frequencies. Similar analysis performed on TS1 revealed that out of four low frequencies obtained at 27, 53, 85 and 77 in TS1, the frequency corresponding to 27 cm^{-1} involving a rotational barrier of 1.65 kcal mol^{-1} acted as hindered rotor and the others were taken as normal vibrational frequencies. On the other hand, in the case of TS2, five low frequencies (16, 24, 58, 70 and 107) were identified as internal rotors. Out of these only one frequency (58 cm^{-1}) involving a rotational barrier of 0.54 kcal mol^{-1} behaved as a hindered rotor and the other three (16, 24 and 107) were treated as free rotors. The remaining frequency at 70 cm^{-1} was treated as a normal vibration. Taking this into account the internal rotation correction to the total partition function was made using the following expression:

$$Q_{vib}^{corr} = \frac{Q_{vib} \cdot Q_{IR}}{\Pi_{Q_{v=i}}}, \quad (4)$$

where Q_{vib} is the harmonic oscillator partition function that includes the contributions due to all the vibrational frequencies, Q_{IR} is internal rotation partition function and $Q_{v=i}$ is the partition function of normal mode vibrations corresponding to internal rotation. In calculating the electronic partition function of Cl care has been taken to account for the splitting of the ground state energy level between ground $^2P_{3/2}$ and excited $^2P_{1/2}$ separated by 881 cm^{-1} due to spin-orbit coupling [34].

The overall rate constant k for the hydrogen atom abstraction reaction of sevoflurane by Cl atom has been calculated by summing up the rate constants corresponding to each reaction channel R1 and R2 and written as:

$$k^{overall} = k_{R1} + k_{R2} \quad (5)$$

The calculated rate constants for reaction R1 (hydrogen atom abstraction from –CHO site) is found to be 1.0×10^{-18} cm^3 $molecule^{-1}$ s^{-1} while that for reaction R2 (hydrogen atom abstraction from $–CH_2F$ site) is 1.13×10^{-13} cm^3 $molecule^{-1}$ s^{-1}. The calculated values show that reaction R1 has negligible contribution and the overall reaction proceeded by H-atom abstraction from the $–CH_2F$ site of the sevoflurane molecule. Our calculated value has very good agreement with the experimental value of $1.10\pm0.1\times10^{-13}$ cm^3 $molecule^{-1}$ s^{-1} determined by Sulbaek Andersen et al. [8]. This result is in accord with the mechanism proposed by Sulbaek Andersen et al. [8] which is based on his experimental observation that Cl-initiated oxidation of sevoflurane occurred with the abstraction of H-atom from the $–CH_2F$ end of the molecule and the resulting products retained the H-atom from the $(CF_3)_2CHO$ site.

Conclusions

We present here the potential energy profile (including geometries, energies and vibrational frequencies of reactant, transition states and products) and kinetic data of H atom abstraction reaction of sevoflurane with Cl atom investigated at the CCSD(T)/6-311G(d,p) level of theory. The barrier height for reaction channels R1 and R2 calculated at CCSD(T) level are found to be 8.8 and 3.4 kcal mol^{-1} respectively. The thermal rate constant for the H atom abstraction of $(CF_3)_2CHOCH_2F$ by Cl atom is found to be 1.13×10^{-13} cm^3 $molecule^{-1}$ s^{-1} at 298 K and 1 atm which is in good agreement with the available experimental data. The results show that reaction channel R2 is the dominant path for the hydrogen atom abstraction. We conclude this study will be helpful in understanding the atmospheric chemistry and estimating the atmospheric life time of sevofluane.

Acknowledgments Authors are thankful to Council of Scientific and Industrial Research (CSIR), New Delhi for providing financial assistance during the course of the present investigation. PKR is thankful to University Grants Commission, New Delhi for providing Rajiv Gandhi National Fellowship (RGNF). Authors are also thankful to UP State Government for providing a grant under its Center of Excellence program and to UGC under SAP program for establishing the computational lab.

References

1. Guenther A, Hewitt CN, Erickson D, Fall R, Geron C, Graedel T, Harley P, Klinger L, Lerdau M, McKay WA, Pierce T, Scholes B, Steinbrecher R, Tallamraju R, Taylor J, Zimmermann P (1995) J Geophys Res 100:8873–8892
2. Sawyer RF, Harley RA, Cadle SH, Norbeck JM, Slott R, Bravo HA (2000) Atoms Environ 34:2161–2181
3. Placet M, Mann CO, Gilbert RO, Niefer MJ (2000) Atoms Environ 34:2183–2204
4. Guenther A, Geron C, Pierce T, Lamb B, Harley P, Fall R (2000) Atoms Environ 34:2205–2230
5. Atkinson R, Arey J (2003) Chem Rev 103:4605–4638
6. Sulbaek Andersen MP, Sander SP, Nielsen OJ, Wagner DS, Sanford TJ Jr, Wallington TJ (2010) Br J Anaesth 105:760–766
7. Wallington TJ, Hurley MD, Fedotov V, Morrell C, Hancock G (2002) J Phys Chem A 106:8391–8398
8. Sulbaek Andersen MP, Nielsen OJ, Karpichev B, Wallington TJ, Sander SP (2012) J Phys Chem A 116:5806–5820
9. Dalmasso P, Taccone R, Nieto J, Teruel M, Lane S (2006) Atmos Environ 40:7298–7307
10. Wingenter OW, Kubo MK, Blake NJ, Smith TW, Blake DR, Rowland FS (1996) J Geophys Res 101:4331–4340
11. Freitas MP, Buhl M, Hagan DO, Cormanich RA, Tormena CF (2012) J Phys Chem A 116:1677–1682
12. Lesarri A, Vega-Toribio A, Suenram RD, Brugh DJ, Grabow JU (2010) Phys Chem Chem Phys 12:9624–9631
13. Tang P, Zubryzcki I, Xu Y (2001) J Comput Chem 22:436–444
14. Truhlar DG (1995) In: Heidrich D (ed) The reaction path in chemistry: current approaches and perspectives. Kluwer, Dordrecht
15. Hu WP, Truhlar DG (1996) J Am Chem Soc 118:860–869
16. Truhlar DG, Garrett BC, Klippenstein SJ (1996) J Phys Chem A 100: 12771–12800
17. Becke AD (1993) J Chem Phys 98:1372–1377
18. Pople JA, Head-Gordon M, Raghavachari K (1987) J Chem Phys 87: 5968–5975
19. Frisch MJ et al. (2010) Gaussian 09 (Version C.01). Gaussian Inc, Wallingford
20. Peng C, Schlegel HB (1993) Isr J Chem 33:449
21. Peng C, Ayala PY, Schlegel HB, Frisch MJ (1996) J Comput Chem 17:49–56
22. Gonzales C, Schlegel HB (1990) J Chem Phys 94:5523–5527
23. Gonzales C, Schlegel HB (1991) J Chem Phys 95:5853–5860
24. Wu Q, Zhu W, Xiao H (2013) J Mol Model 19:2945–2954
25. Lide DR (ed) (1994) CRC Handbook of Chemistry and Physics, 75th edn. CRC, New York
26. Fischer H, Radom L (2001) Angew Chemie Int Ed 40:1340–1371
27. Sun H, Gong H, Pan X, Hao L, Sun CC, Wang R, Huang X (2009) J Phys Chem A 113:5951–5957

28. Song G, Jia X, Gao Y, Luo J, Yu Y, Wang R, Pan X (2010) J Phys Chem A 114:9057–9068
29. Johnson RD (ed) (2011) NIST Computational Chemistry Comparison and Benchmark Database, NIST Standard Reference Database 101, Release 15b, August 2011. http://cccbdb.nist.gov/
30. Frisch A, Nielsen AB, Holder AJ et al. (2009) Gauss-View 05. Gaussian Inc, Wallingford, CT
31. Laidler KJ (2004) Chemical Kinetics, 3rd edn. Pearson Education, New Delhi
32. Truhlar DG, Garrett BC, Klippenstein SJ (1996) J Phys Chem 100: 12771–12800
33. Wigner EP (1932) Z Phys Chem B19:203–216
34. Chase MW Jr, Davies CA, Downey JR Jr, Frurip DJ, McDonald RA, Syverud AN (1985) JANAF thermochemical tables. J Phys Chem Ref Data 14: Suppl 1, 3rd edn